PCCP

Cite this: *Phys. Chem. Chem. Phys.*, 2012, **14**, 4964–4970

www.rsc.org/pccp

PAPER

Brownian dynamics simulation study on the self-assembly of incompatible star-like block copolymers in dilute solution

Bin Li, You-Liang Zhu, Hong Liu* and Zhong-Yuan Lu*

Received 8th December 2011, Accepted 17th February 2012
DOI: 10.1039/c2cp23932a

We study the self-assembly of symmetric star-like block copolymers $(A_x)_y(B_x)_yC$ in dilute solution by using Brownian dynamics simulations. In the star-like block copolymer, incompatible A and B components are both solvophobic, and connected to the center bead C of the polymer. Therefore, this star-like block copolymer can be taken as a representative of soft and deformable Janus particles. In our Brownian dynamics simulations, these "soft Janus particles" are found to self-assemble into worm-like lamellar structures, loose aggregates and so on. By systematically varying solvent conditions and temperature, we build up the phase diagram to illustrate the effects of polymer structure and temperature on the aggregate structures. At lower temperatures, we can observe large worm-like lamellar aggregates. Upon increasing the temperature, some block copolymers detach from the aggregate; this phenomenon is especially sensitive for the polymers with less arms. The aggregate structure will be quite disordered when the temperature is high. The incompatibility between the two parts in the star-like block copolymer also affects the self-assembled structures. We find that the worm-like structure is longer and narrower as the incompatibility between the two parts is stronger.

1 Introduction

Nowadays, considerable interest has arisen in the self-assembly of anisotropic particles, such as patchy, multicompartment and Janus particles.[1–5] The anisotropic particles have shown great potential for applications in the fields of drug delivery,[6] emulsions[7,8] and others. In recent years, Glotzer and co-workers[9–12] had successfully proposed many kinds of interesting nanostructures *via* self-assembly of patchy particles by using Brownian dynamics simulations. Janus particles (named after the two-faced Roman God Janus) could be considered as a special class of patchy particles. The concept of "Janus particles" was originally raised by de Gennes in his Nobel Prize lecture,[13] which describes one type of particles with two equal surface areas possessing different properties,[14] such as hydrophobic/hydrophilic, charged/uncharged, and many others. Because of their particular nature, a series of novel materials *via* oriented assembly of Janus particles have been discovered.

The literature includes a variety of ways to prepare, synthesize, and self-assemble Janus particles.[15–20] Granick and coworkers had found many kinds of novel structures using rigid Janus spheres in experiments and *via* simulations.[21–26] Müller and coworkers used block copolymers to design Janus particle structures and obtained many kinds of nanostructures, such as Janus micelles, Janus cylinders, Janus discs and other novel structures.[27–33]

The star-like polymers had been used to represent Janus particles in experiments and simulations.[34,35] According to the work of Likos and coworkers about the structures and properties of the dendritic macromolecules in various solvents,[36–39] the star-like polymers which have enough arms could be viewed as colloidal particles under some specific solvents. Thus in this work, we consider star-like *block* copolymers which contain two types of arms to describe one kind of soft Janus particles. Because of the incompatibility between the two types of components, microphase separation could be expected to occur in the star-like molecule, thus the structure of Janus particle can be formed. This type of Janus particles is deformable due to their softness; and the structure of the Janus particles can be largely influenced by changing solvent conditions and temperature. As a consequence, the mechanism of the self-assembly of soft Janus particles will have additional entropic consideration due to chain conformation, in addition to typical enthalpic effects that dominate the self-assembly of rigid Janus particles.[40–43] Motivated by these, here we study the self-assembly of star-like block copolymers (representing soft Janus particles) *via* Brownian dynamics simulations. The influences of arm number, solvent condition, and incompatibility between the components are scrutinized in detail.

The paper is organized as follows: Section 2 exhibits the model of star-like block copolymers and the Brownian dynamics

Institute of Theoretical Chemistry, State Key Laboratory of Theoretical and Computational Chemistry, Jilin University, Changchun 130023, China.
E-mail: hongliu@jlu.edu.cn, luzhy@jlu.edu.cn

simulation details, Section 3 shows the results and the corresponding discussion, and finally, Section 4 presents the concluding remarks.

2 Model and method

We use a coarse-grained model to represent the star-like block copolymers, as illustrated schematically in Fig. 1. In this work, we adopt many linear chains connected to a center bead to form a star-like block copolymer $(A_x)_y(B_x)_yC$, where both A and B are solvophobic beads, and C is the center bead. Each star-like polymer contains $N_b = 2xy + 1$ beads, in which x is the length of each arm, and y is the number of arms which exclusively contain either A or B type beads. We fix the number of beads $x = 10$ in each arm, and change the number of arms to characterize different star-like block copolymer structures.

The non-bonded interactions between the coarse-grained beads are represented by Lennard–Jones (LJ) potential,

$$U_{\mathrm{LJ}} = \begin{cases} 4\varepsilon\left[\left(\frac{\sigma}{r}\right)^{12} - \left(\frac{\sigma}{r}\right)^{6}\right], & r \le r_{\mathrm{cut}} \\ 0, & r > r_{\mathrm{cut}} \end{cases} \quad (1)$$

in which ε and σ are the well depth and the bead diameter, respectively. Here r is the distance between two beads, and $r_{\mathrm{cut}} = 3.0\sigma$ is the cutoff distance beyond which the LJ potential is equal to 0. For simplicity, all the beads in the system have the same size σ and mass m. The time unit is $\tau = \sigma\sqrt{m/\varepsilon}$. All the parameters used in this work are in reduced units with basic units being ε, σ, m, and τ.

The Brownian dynamics (BD) simulation technique was proven to be a suitable and efficient method in the studies of self-assembly of Janus particles.[9,10,44–46] In Brownian dynamics, the equation of motion of each bead in the system is governed by Langevin equation

$$m_i\ddot{\mathbf{r}}_i(t) = \mathbf{F}_i^C(\mathbf{r}_i(t)) + \mathbf{F}_i^R(t) - \gamma_i\mathbf{v}_i(t) \quad (2)$$

where v is the velocity of the bead, $\gamma = k_{\mathrm{B}}T/D$ is the friction coefficient, and D is the diffusion coefficient. We assume that there are no spatial or temporal fluctuations of friction coefficient and fix $\gamma = 1.0$. The effect of solvents is implicitly treated by the random force which satisfies the fluctuation-dissipation theorem,

$$\langle \mathbf{F}_i^R(t)\mathbf{F}_j^R(t')\rangle = 6\gamma k_{\mathrm{B}}T\delta_{ij}\delta(t - t') \quad (3)$$

where k_{B} is the Boltzmann constant and T the temperature. The coupling between friction and random forces acts as an effective thermostat.

The simulations are performed in an NVT ensemble in a cubic box under periodic boundary conditions. We set the box side length as 100, and control the number density of coarse-grained beads at 0.05, so the number of coarse-grained beads in the simulation box is 5×10^4. We fix $\varepsilon_{\mathrm{AA}} = \varepsilon_{\mathrm{BB}} = 1.0$ to describe the effective interactions between the beads of the same type, and $\varepsilon_{\mathrm{AC}} = \varepsilon_{\mathrm{BC}} = 1.0$ to describe the interaction between the center bead and the arm beads. The only parameter that can be varied in our BD simulations is $\varepsilon_{\mathrm{AB}}$, which takes a value smaller than 1.0 for representing unfavorable interactions between A and B type beads. This is because when the well depth of $\varepsilon_{\mathrm{AB}}$ is shallower than $\varepsilon_{\mathrm{AA}}(= \varepsilon_{\mathrm{BB}})$, the attraction between A and B type beads is weaker than that between the same type.[47] For suitable $\varepsilon_{\mathrm{AB}} < 1.0$, microphase separation between A and B components will occur in each molecule and a soft Janus particle can be formed. Thus in this research, we are considering a symmetric case with equal composition and balanced interactions between A and B type beads.

The polymer chains are constructed by connecting adjacent beads together with harmonic bond potential,

$$U_{\mathrm{bond}} = \tfrac{1}{2}k(r - r_0)^2 \quad (4)$$

where r_0 is the equilibrium bond length, and k is the spring force constant. Here we set $k = 40.0$ and $r_0 = 1.0$. A time step of $\delta t = 0.01$ is used, and the total simulation steps are 3×10^7–6×10^7. All simulations are performed with HOOMD[48,49] on Nvidia Tesla C2050 GPU.

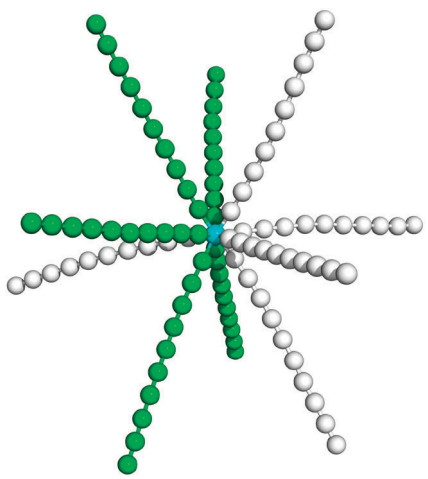

Fig. 1 The representative architecture of star-like block copolymers with 10 arms. There are 10 beads in each arm, with green and white beads representing A and B components, respectively, and cyan bead representing the center bead C.

3 Results and discussion

In the studies of self-assembly of dendritic molecules using BD simulations,[50,51] $T^* = k_{\mathrm{B}}T/\varepsilon = 1.8$ was identified as the lowest temperature at which the balance between the aggregated and free molecules could be maintained. Therefore in this research, we set $T^* = 1.8$ in most of the BD simulations. Firstly we consider the star-like block copolymer with 40 arms. The non-bonded interaction parameter $\varepsilon_{\mathrm{AB}} = 0.5$ is set for representing the effective repulsion between A and B type beads. The incompatibility between A and B type beads is stronger as $\varepsilon_{\mathrm{AB}}$ is smaller, which may be experimentally tuned by adding nonsolvent or changing the pH value.

In order to characterize the self-assembly process and the final structure, we calculate the orientation order parameter Q,[52,53]

$$Q = \frac{2}{(N-1)N}\left\langle \sum_i \sum_{j>i} \frac{1}{2}(3\cos^2\theta_{ij} - 1) \right\rangle \quad (5)$$

where N is the number of star-like block copolymers in the system, θ_{ij} is the angle between the unit vectors **i** and **j**, which, respectively, connects the centers of mass of the two parts in a

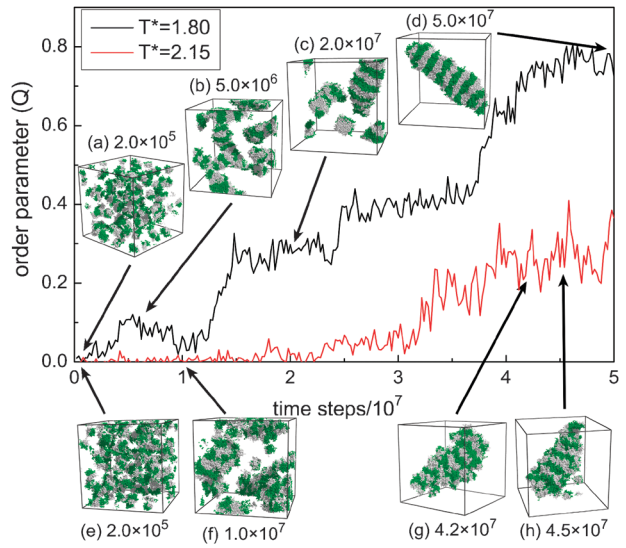

Fig. 2 The time evolution of order parameter Q at $T^* = 1.80$ and $T^* = 2.15$, respectively. The snapshots are chosen to highlight the possible self-assembly structures at different kinetic stages.

soft Janus particle. Note that $\theta_{ij} = 0$ corresponds to $Q = 1$, which reflects perfectly ordered structure, whereas a random orientation of **i** results in $Q = 0$.

Fig. 2 shows the time evolution of orientation order parameter Q for $(A_{10})_{20}(B_{10})_{20}C$ block copolymers at $T^* = 1.80$ and $T^* = 2.15$, respectively, together with some representative snapshots for highlighting typical self-assembly structures. At $T^* = 1.80$, in the beginning of the simulations, the star-like block copolymers collapse to form single-molecule spherical globules since the solvent is bad for both components of the block copolymers. Then microphase separation between A and B components occurs due to the incompatibility between the two parts, and single-molecule soft Janus particles are formed. Fig. 2(a) shows the snapshot at 2.0×10^5 time steps, at which Q is close to 0, reflecting that the Janus particles are randomly oriented. Subsequently, the Janus particles start to aggregate and some small clusters with lamellar structures are formed (for example, as shown in Fig. 2(b)), as a consequence, the order parameter gradually increases to a larger value. At about 1.2×10^7 time steps, the small clusters continue to merge with larger lamellar aggregates (typical snapshot is shown in Fig. 2(c)) and the order parameter rapidly increases and reaches a plateau value. At about 3.8×10^7 time steps, the larger lamellar aggregates continue to coalesce with Q increasing rapidly, finally a large lamellar worm-like aggregate is formed (typical snapshot is shown in Fig. 2(d), at which Q has a new plateau value about 0.75, reflecting a highly ordered structure). The kinetic pathway for the self-assembly of $(A_{10})_{20}(B_{10})_{20}C$ block copolymers at $T^* = 1.80$ is reflected by a step-by-step fashion. At different stages (*i.e.*, plateaus in Fig. 2), the aggregates are always characterized by lamellar worm-like structures, but their sizes and orientations are different at different kinetic stages. Therefore in experiments, it might be possible to produce lamellar worm-like structures with controllable sizes by controlling the kinetic conditions during the self-assembly process of star-like block copolymers at lower temperatures.

We then consider the temperature influence on the self-assembly process and possible structures of $(A_{10})_{20}(B_{10})_{20}C$ block copolymers. Fig. 2 also shows the time evolution of Q for $(A_{10})_{20}(B_{10})_{20}C$ block copolymers at $T^* = 2.15$, together with some representative aggregate structures. Apparently, the time evolution of Q at $T^* = 2.15$ is quite different from that at $T^* = 1.80$. In the beginning of the simulation at $T^* = 2.15$, Q is close to 0, which characterizes random orientation of star-like block copolymers (typical snapshot can be seen in Fig. 2(e)). Then Q fluctuates around 0 for quite a long time (about 3.0×10^7 time steps). In this period, the star-like block copolymers gradually aggregate to form large cluster structures, but there is no overall orientation of the star-like block copolymers inside the clusters (as shown in Fig. 2(f)). Thus Q is very small in this period, in contrast to the kinetic pathway for Q at $T^* = 1.80$. Subsequently, microphase separation takes place in the large aggregate formed by these block copolymers, and lamellar domains can be observed, as shown in Fig. 2(g) and (h) for the snapshots at 4.2 and 4.5×10^7 time steps, respectively. The order parameter for the equilibrium structure at $T^* = 2.15$ is only about 0.3, which reflects that the layers in the worm-like structure are not as regular as those at $T^* = 1.80$.

We also calculate the weight average aggregate weight $\bar{M}_w$ at both $T^* = 1.80$ and 2.15. $\bar{M}_w$ can be calculated by

$$\bar{M}_w = \frac{\sum_i N_i M_i^2}{\sum_i N_i M_i} \qquad (6)$$

where N_i is the number of aggregates of molecular weight M_i. The time evolution of $\bar{M}_w$ is shown in Fig. 3. At $T^* = 1.80$, there are several stages of $\bar{M}_w$ during the simulation: at the beginning, the Janus particles start to aggregate so the value of $\bar{M}_w$ increases rapidly; after several aggregates are formed, $\bar{M}_w$ is stable until 1.5×10^7 time steps; when the aggregates merge together, $\bar{M}_w$ reaches about 5×10^4 because a large aggregate is formed. This also reflects a step-by-step kinetic pathway at $T^* = 1.80$, and the time steps at which $\bar{M}_w$ jumps are in accordance with the jumps of orientation order parameter Q at $T^* = 1.80$ in Fig. 2. At $T^* = 2.15$, there are large fluctuations in the beginning of the simulation, because the aggregates will

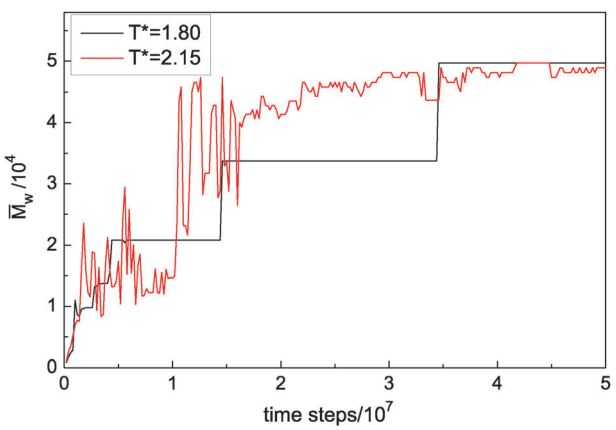

Fig. 3 The time evolution of weight average aggregate weight $\bar{M}_w$ in the system at $T^* = 1.80$ and $T^* = 2.15$.

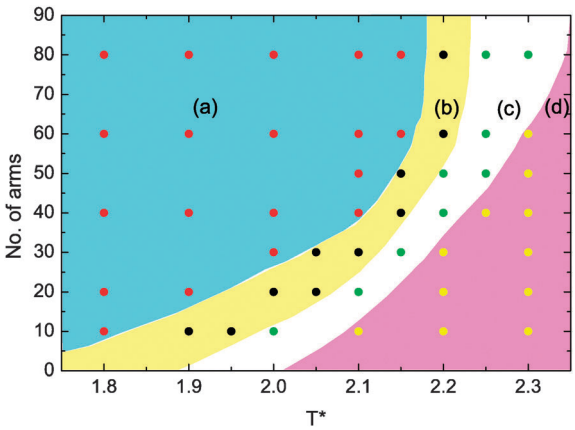

Fig. 4 Phase diagram of star-like block copolymers. In the simulations, $\varepsilon_{AA} = \varepsilon_{BB} = 1$, $\varepsilon_{AB} = 0.5$. The symbols are the simulation results, and the colored domains are drawn schematically to guide the eye.

split into smaller ones due to high temperature. $\bar{M}_w$ is stable after 1.5×10^7 time steps, which reflects a large aggregate with some smaller ones. This time is lesser than that by which orientation order parameter Q begins to increase (at about 3.0×10^7 time steps), thus the Janus particles are oriented randomly in the large aggregate between 1.5×10^7 and 3.0×10^7 time steps.

From the time evolution of Q and $\bar{M}_w$ at these two temperatures we can find that the kinetic pathways for the self-assembly of star-like block copolymers are different: when the temperature is low, the formation of lamellar structure and the aggregation of the star-like block copolymers occur simultaneously; but when the temperature is higher, the lamellar structure can be observed only after the formation of large aggregates.

We also examine the influence of the number of arms in star-like block copolymers on the self-assembled structures at different temperatures. Fig. 4 shows the schematic phase diagram with the number of arms plotted with T^*. Region (a) in Fig. 4 denotes the condition that worm-like aggregates with clear lamellar structures can be observed, and region (d) denotes the condition that only disordered structures exist. Between these regions, there are two intermediate regions (b) and (c), denoting the conditions for observing worm-like aggregates in equilibrium with star-like block copolymers and aggregates without clear lamellar structures, respectively. Similar to the results of Sciortino and co-workers,[54] ordered structures are easily generated at lower temperatures. It is obvious that the star-like block copolymers with more arms self-assemble into a large lamellar aggregate more easily at suitable temperatures. For example, at $T^* = 2.15$, the star-like block copolymers with 80 arms generate a large worm-like lamellar structure, whereas the polymers with 30 arms can only generate structures without clear layers. The number of contacting pairs in a cutoff distance between two approaching star-like block copolymers plays a key role here. For the star-like block copolymers with more arms, the number of contacting pairs between two star-like block copolymers at certain distances will be larger than that of the polymers with less arms. As a consequence, the Lennard–Jones attractive

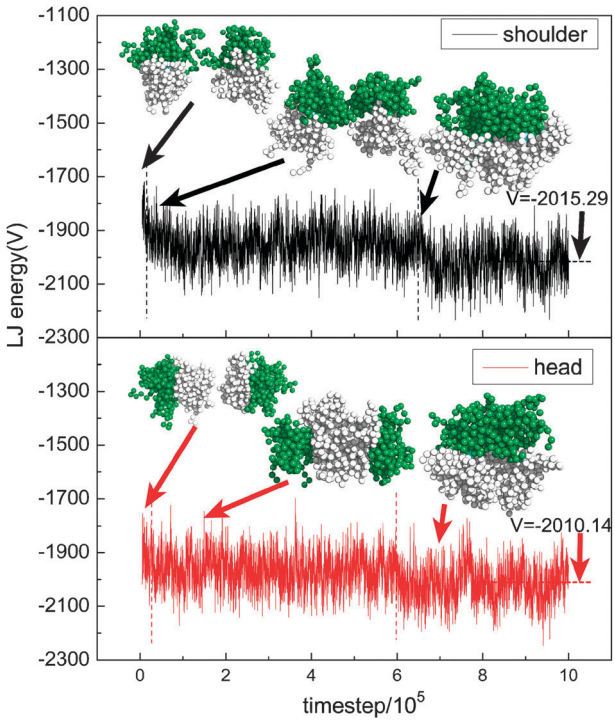

Fig. 5 The time evolution of the LJ potential energy during two star-like block copolymers approaching from shoulder-by-shoulder and head-to-head directions, respectively. The representative snapshots are taken at different packing stages. The vertical dash lines indicate the periods with different packing configurations, and the horizontal dash lines indicate the mean value of the potential energy after the two copolymers aggregate together.

interactions between the polymers with more arms will be larger, and these polymers can easily form large aggregates. Therefore, as reflected in Fig. 4, for the star-like block copolymers with less arms, we have to decrease the temperature to observe worm-like lamellar structures.

The self-assembly of these star-like block copolymers (namely, the soft and deformable Janus particles) is characterized by apparent lamellar structures at a molecular length scale. This can be attributed to the deformability of the soft Janus particles. As shown in Fig. 5, we can see that there is no energy difference for two soft Janus particles approaching each other in head-to-head or shoulder-by-shoulder directions. In these packing configurations, the chains can easily stretch out and take new conformations to maximize the contact between the two soft Janus particles. On the contrary, the attractive energy will be smaller if the two soft Janus particles approach in other directions. Therefore, the soft Janus particles tend to pack into lamellar structures at suitable temperatures. For comparison, we have also studied the self-assembly of rigid Janus particles under the same thermodynamic conditions. The structure of the rigid Janus particle is shown in Fig. 6. There are 443 beads in each Janus particle. The radius of the Janus particle is 4σ, which is similar to the radius of gyration of star-like block copolymers with 40 arms in poor solvents. The shape and rigidness of the Janus particle are maintained by the rigid body built of beads in the HOOMD package.[55] The box side length is also 100, and the number of Janus particles is the

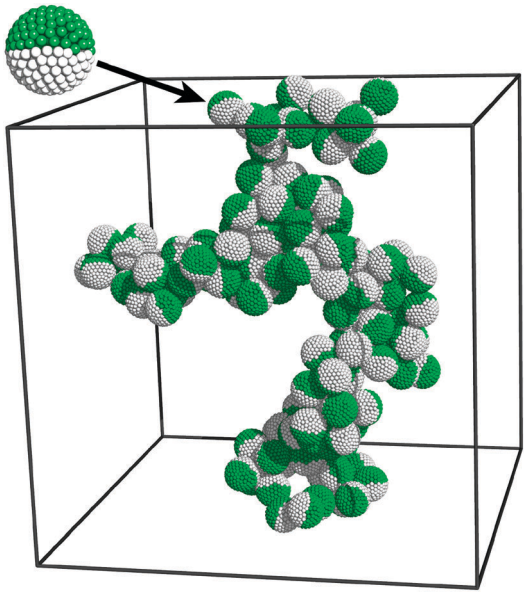

Fig. 6 The structure of aggregates assembled by the Janus particles, the model of rigid Janus particle is at the top left corner of the figure and it is composed of two kinds of beads which have equal surfaces.

same as the number of star-like block copolymers with 40 arms. All the parameters are set to the same as those of the star-like block copolymers.

The snapshot of the equilibrium structure assembled by the rigid Janus particles is shown in Fig. 6. Unlike the soft Janus particles formed by star-like block copolymers, the structure assembled by the rigid Janus particles is not the lamellar aggregate. Actually it is quite similar to the structures obtained by Granick and co-workers.[21,22] There is no deformability in the rigid Janus particles, so the Janus particles access each other from all possible orientations to maximize the contact and satisfy the dense packing.[56]

To find out the influence of compatibility between the two components of block copolymers on the self-assembly structures, we focus on $T^* = 1.80$ and perform a series of simulations at different ε_{AB}. In order to describe the shape of the aggregates assembled by the star-like block copolymers, we calculate the ratio of length to width of the aggregates. The radius of gyration tensor is[57,58]

$$A = \begin{bmatrix} S_{xx} & S_{xy} & S_{xz} \\ S_{yx} & S_{yy} & S_{yz} \\ S_{zx} & S_{zy} & S_{zz} \end{bmatrix} \qquad (7)$$

with $S_{xx} = \frac{1}{n}\sum_{i=1}^{n}(x_i - x_{cm})(x_i - x_{cm})$, $S_{xy} = \frac{1}{n}\sum_{i=1}^{n}(x_i - x_{cm})(y_i - y_{cm})$, and so on. Here n is the total number of beads in an aggregate, r_i is the position of each bead, and x_{cm} is the x coordinate of center of mass of the aggregate. We can obtain three eigenvalues λ_1, λ_2, and λ_3 *via* Jacobian transformation of matrix A. The ratio of length to width of the aggregate (η) is defined by the largest value of the three eigenvalues divided by the smallest one. We also calculate the asphericity parameter

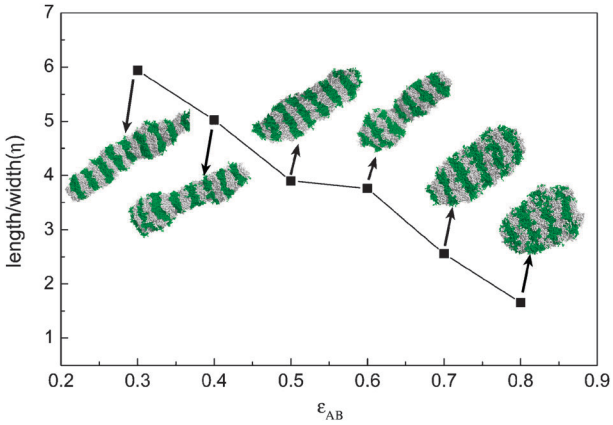

Fig. 7 The dependence of length to width ratios of the self-assembly structures on the incompatibility of the two components. Typical equilibrium lamellar structures are also shown.

of the star-like block copolymer at $T^* = 1.80$ but with different ε_{AB}. The asphericity parameter δ can be defined by

$$\delta = \frac{(\alpha_1^2 - \alpha_2^2)^2 + (\alpha_1^2 - \alpha_3^2)^2 + (\alpha_2^2 - \alpha_3^2)^2}{2(\alpha_1^2 + \alpha_2^2 + \alpha_3^2)^2} \qquad (8)$$

where α_i denotes the eigenvalues of radius of gyration tensor for a *single* star-like block copolymer. The shape of the polymer is close to a sphere when this value is close to 0, whereas it denotes a stick when this value is close to 1.

Fig. 7 shows the length to width ratios *versus* ε_{AB} and the corresponding self-assembly structures for star-like block copolymers with 40 arms. The length to width ratio of the self-assembly structure η decreases gradually from 6.0 to 1.7 with increasing ε_{AB}. Because smaller ε_{AB} corresponds to stronger incompatibility between the two block copolymer components, thus from Fig. 7 we can find that the worm-like lamellar structures strongly correlate to the incompatibility between the block copolymer components. The results of asphericity parameters for star-like block copolymers with different ε_{AB} are shown in Table 1. Apparently, the incompatibility between A and B components will be stronger in the case with smaller ε_{AB}, as a result, the shape of the star-like block copolymer will deviate from spherical more and more and turn to be peanut-like, correspondingly, the asphericity parameter will be larger. For two peanut-like molecules approaching each other, the number of contacting pairs will be smaller from the shoulder-by-shoulder direction as compared to that from the head-to-head direction, so the self-assembly structures tend to be long and narrow. If ε_{AB} is larger, *i.e.*, the soft Janus particles are more spherical, there is basically no energy difference for the two molecules approaching from the shoulder-by-shoulder direction or from the head-to-head direction. As a consequence, the length to width ratios of self-assembly structures in the cases of larger ε_{AB} will be smaller. It implies that, in experiment, the components of the star-like block copolymers could be modified to control the morphology of the worm-like lamellar structures.

The radial distribution function $g(r)$ of the centers of mass of the two parts in the soft Janus particles is also calculated to characterize the morphology of the lamellar aggregates.

Table 1 The asphericity parameter δ of a single star-like block copolymer at different ε_{AB} (unit: 10^{-2})

ε_{AB}	0.3	0.4	0.5	0.6	0.7	0.8
δ	1.622	1.494	1.375	1.299	1.189	1.108

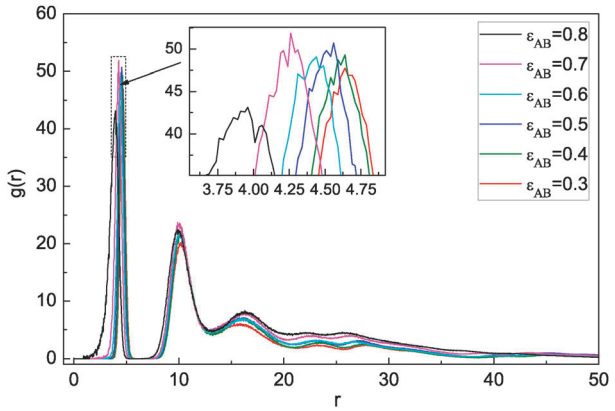

Fig. 8 The radial distribution function of the centers of mass of the two components in a block copolymer at $T^* = 1.80$ but with different ε_{AB}. The inset shows the positions of the first peaks.

This function gives the probability of finding a pair of centers of mass of the two parts in the soft Janus particles with a distance r apart, and is defined by,[59]

$$g(r) = \frac{V}{N^2}\left\langle \sum_i \sum_{j \neq i} \delta(r - r_{ij}) \right\rangle \quad (9)$$

where N is the total number of centers of mass of the two parts in the soft Janus particles in the system and V is the volume of the simulation box. The results of $g(r)$ at different ε_{AB} are shown in Fig. 8. The positions of the first peaks of $g(r)$ appear at r from 3.8 to 4.8, which indicate the distance between the centers of mass of the two parts in a soft Janus particle. The position of the first peak decreases with increasing ε_{AB}, since the distance between the two centers of mass is smaller with the incompatibility between the two copolymer components being weaker. The second peaks of $g(r)$ appear at about 10.0 which is roughly twice than that of the first peaks. This value actually indicates the distance between the centers of mass of components for two Janus particles approaching from the head-to-head direction. The distribution of the peaks of $g(r)$ clearly shows the lamellar structures of the aggregates.

4 Conclusions

In this work, we have obtained soft Janus particles *via* microphase separation of star-like block polymers with two kinds of incompatible arms. In the cases that the two components are strongly incompatible, the Janus particles deform to peanut shape due to their softness. A series of nanostructures are formed under different thermodynamic conditions. The characteristic lamellar worm-like structures can be assembled *via* the aggregation of soft Janus particles because of their deformability and softness. The morphology of the structures can also be influenced by the incompatibility between the two components, especially for the block copolymer with less arms. Our simulation of this kind of soft Janus particle may provide a new route to study the self-assembly of Janus particles and design novel structures.

Acknowledgements

This work is supported by National Science Foundation of China (21025416, 20974040, 50930001) and China Postdoctoral Science Foundation (20110491295).

References

1 S. C. Glotzer, *Science*, 2004, **306**, 419–420.
2 S. C. Glotzer and J. A. Anderson, *Nat. Mater.*, 2010, **9**, 885–887.
3 A. B. Pawar and I. Kretzschmar, *Macromol. Rapid Commun.*, 2010, **31**, 150–168.
4 J. Du and R. K. O'Reilly, *Chem. Soc. Rev.*, 2011, **40**, 2402–2416.
5 E. Bianchi, R. Blaak and C. N. Likos, *Phys. Chem. Chem. Phys.*, 2011, **13**, 6397–6410.
6 J. A. Champion, Y. K. Katare and S. Mitragotri, *Proc. Natl. Acad. Sci. U. S. A.*, 2007, **104**, 11901–11904.
7 N. Glaser, D. J. Adams, A. Böker and G. Krausch, *Langmuir*, 2006, **22**, 5227–5229.
8 J. W. Kim, D. Lee, H. C. Shum and D. A. Weitz, *Adv. Mater.*, 2008, **20**, 3239–3243.
9 Z. Zhang, M. A. Horsch, M. H. Lamm and S. C. Glotzer, *Nano Lett.*, 2003, **3**, 1341–1346.
10 Z. Zhang and S. C. Glotzer, *Nano Lett.*, 2004, **4**, 1407–1413.
11 Z. Zhang, A. S. Keys, T. Chen and S. C. Glotzer, *Langmuir*, 2005, **21**, 11547–11551.
12 S. C. Glotzer and M. J. Solomon, *Nat. Mater.*, 2007, **6**, 557–562.
13 P. G. de Gennes, *Rev. Mod. Phys.*, 1992, **64**, 645–648.
14 F. Wurm and A. F. M. Kilbinger, *Angew. Chem., Int. Ed.*, 2009, **48**, 8412–8421.
15 A. Perro, S. Reculusa, S. Ravaine, E. Bourgeat-Lami and E. Duguet, *J. Mater. Chem.*, 2005, **15**, 3745–3760.
16 C. Singh, P. K. Ghorai, M. A. Horsch, A. M. Jackson, R. G. Larson, F. Stellacci and S. C. Glotzer, *Phys. Rev. Lett.*, 2007, **99**, 226106.
17 E. B. Mock and C. F. Zukoski, *Langmuir*, 2011, **26**, 13747–13750.
18 N. P. Pardhy and B. M. Budhlall, *Langmuir*, 2011, **26**, 13130–13141.
19 T. Tanaka, M. Okayama, H. Minami and M. Okubo, *Langmuir*, 2011, **26**, 11732–11736.
20 Y. Li, W. B. Zhang, I. F. Hsieh, G. Zhang, Y. Cao, X. Li, C. Wesdemiotis, B. Lotz, H. Xiong and S. Z. D. Cheng, *J. Am. Chem. Soc.*, 2011, **133**, 10712–10715.
21 L. Hong, A. Cacciuto, E. Luijten and S. Granick, *Nano Lett.*, 2006, **6**, 2510–2514.
22 L. Hong, A. Cacciuto, E. Luijten and S. Granick, *Langmuir*, 2008, **24**, 621–625.
23 S. Jiang, M. J. Schultz, Q. Chen, J. S. Moore and S. Granick, *Langmuir*, 2008, **24**, 10073–10077.
24 S. Jiang and S. Granick, *Langmuir*, 2008, **24**, 2438–2445.
25 S. M. Anthony, M. Kim and S. Granick, *Langmuir*, 2008, **24**, 6557–6561.
26 Q. Chen, J. K. Whitmer, S. Jiang, S. C. Bae, E. Luijten and S. Granick, *Science*, 2011, **331**, 199–202.
27 R. Erhardt, M. Zhang, A. Böker, H. Zettl, C. Abetz, P. Frederik, G. Krausch, V. Abetz and A. H. E. Müller, *J. Am. Chem. Soc.*, 2003, **125**, 3260–3267.
28 Y. Liu, V. Abetz and A. H. E. Müller, *Macromolecules*, 2003, **36**, 7894–7898.
29 A. Walther, X. André, M. Drechsler, V. Abetz and A. H. E. Müller, *J. Am. Chem. Soc.*, 2007, **129**, 6187–6198.
30 A. Walther, K. Matussek and A. H. E. Müller, *ACS Nano*, 2008, **2**, 1167–1178.
31 A. Walther, M. Drechsler, S. Rosenfeldt, L. Harnau, M. Ballauff, V. Abetz and A. H. E. Müller, *J. Am. Chem. Soc.*, 2009, **131**, 4720–4728.
32 A. Walther, C. Barner-Kowollik and A. H. E. Müller, *Langmuir*, 2010, **26**, 12237–12246.

33 T. M. Ruhland, A. H. Gröschel, A. Walther and A. H. E. Müller, *Langmuir*, 2011, **27**, 9807–9814.
34 A. Kiriy, G. Gorodyska, S. Minko, M. Stamm and C. Tsitsilianis, *Macromolecules*, 2003, **36**, 8704–8711.
35 Y. Chang, W. C. Chen, Y. J. Sheng, S. Jiang and H. K. Tsao, *Macromolecules*, 2005, **38**, 6201–6209.
36 C. N. Likos, H. Löwen, M. Watzlawek, B. Abbas, O. Jucknischke, J. Allgaier and D. Richter, *Phys. Rev. Lett.*, 1998, **80**, 4450–4453.
37 M. Ballauff and C. N. Likos, *Angew. Chem., Int. Ed.*, 2004, **43**, 2998–3020.
38 C. N. Likos, *Soft Matter*, 2006, **2**, 478–498.
39 S. Huissmann, R. Blaak and C. N. Likos, *Macromolecules*, 2009, **42**, 2806–2816.
40 P. Ziherl and R. D. Kamien, *J. Phys. Chem. B*, 2001, **105**, 10147–10158.
41 G. Ungar, Y. Liu, X. Zeng, V. Percec and W. D. Cho, *Science*, 2003, **299**, 1208–1211.
42 T. B. Martin, A. Seifpour and A. Jayaraman, *Soft Matter*, 2011, **7**, 5952–5964.
43 C. R. Iacovella, A. S. Keys and S. C. Glotzer, *Proc. Natl. Acad. Sci. U. S. A.*, 2011, **108**, 20935–20940.
44 M. A. Horsch, Z. Zhang and S. C. Glotzer, *Phys. Rev. Lett.*, 2005, **95**, 056105.
45 C. R. Iacovella, M. A. Horsch, Z. Zhang and S. C. Glotzer, *Langmuir*, 2005, **21**, 9488–9494.
46 C. R. Iacovella, M. A. Horsch and S. C. Glotzer, *J. Chem. Phys.*, 2008, **129**, 044902.
47 D. F. Parsons and D. R. M. Williams, *Phys. Rev. Lett.*, 2007, **99**, 228302.
48 HOOMD-blue web page: http://codeblue.umich.edu/hoomd-blue.
49 J. A. Anderson, C. D. Lorenz and A. Travesset, *J. Comput. Phys.*, 2008, **227**, 5342–5359.
50 N. W. Suek and M. H. Lamm, *Langmuir*, 2008, **24**, 3030–3036.
51 C. Georgiadis, O. Moultos, L. N. Gergidis and C. Vlahos, *Langmuir*, 2011, **27**, 835–842.
52 B. Fodi and R. Hentschke, *J. Chem. Phys.*, 2000, **112**, 6917–6924.
53 Z. W. Li, L. J. Chen, Y. Zhao and Z. Y. Lu, *J. Phys. Chem. B*, 2008, **112**, 13842–13848.
54 F. Sciortino, A. Giacometti and G. Pastore, *Phys. Rev. Lett.*, 2009, **103**, 237801.
55 T. D. Nguyen, C. L. Phillips, J. A. Anderson and S. C. Glotzer, *Comput. Phys. Commun.*, 2011, **182**, 2307–2313.
56 V. N. Manoharan, M. T. Elsesser and D. J. Pine, *Science*, 2003, **301**, 483–487.
57 J. Rudnick and G. Gaspari, *J. Phys. A: Math. Gen.*, 1986, **19**, L191–L193.
58 C. M. Lin, Y. Z. Chen, Y. J. Sheng and H. K. Tsao, *React. Funct. Polym.*, 2009, **69**, 539–545.
59 M. P. Allen and D. J. Tildesley, *Computer Simulation of Liquids*, Oxford University Press, 1987.

